Broadband, Beam-Steering Asymmetric Stacked Microstrip Phased Array with Enhanced Front-to-Back Ratio

Melih Türk [1] and Fikret Tokan [2]

[1] The Scientific and Technological Research Council of Turkey, Gebze, 41470, Kocaeli, Turkey
melih.turk@tubitak.gov.tr

[2] Department of Electronics and Communications Engineering, Faculty of Electrical and Electronics
Yildiz Technical University, Istanbul, Turkey
ftokan@yildiz.edu.tr

Abstract ─ The backward radiation is a critical problem that may cause breakdown of the front-end circuits that are integrated behind the antenna. Thus, antennas having high Front to Back Ratio (FBR) are required. For phased arrays, the back lobe suppression is required for all scanning angles at all frequencies of the band. In this work, a stacked patch linear array with asymmetric configuration is proposed. It is capable of scanning the beam in $\pm 40^{o}$ with less than 1.34 dB scanning loss. Due to the usage of probe-fed stacked patches as the antenna elements, impedance matching in 8-10 GHz is achieved. More than 30 dB FBR is obtained for broadside radiation. It is above 20 dB when the beam is steered to $\theta = 40^{o}$. This is valid for all frequencies of the band. A prototype is fabricated and measured. Higher than 38 dB FBR is observed. With its broadband, high FBR and low scanning loss, the proposed asymmetrical stacked patch phased array is suitable as radar and base station antenna.

Index Terms ─ Back-lobe suppression, front to back ratio, linear phased array, stacked patch, wideband antenna.

I. INTRODUCTION

Microstrip antenna arrays are popular solutions for wide beam scanning function that is essential in radar, electronic warfare and communication systems. Wide frequency coverage, ease of fabrication and conformity are key parameters for the success of these systems. Among feeding structures, probe-fed solution is widely used due to its robust nature and impedance matching performance [1]. However, narrow band characteristic of a microstrip antenna is a major drawback for wide band applications. There has been considerable interest towards designing wideband microstrip antennas to be used in phased arrays for wide beam scanning. It is proved that thick laminates with low dielectric constant is likely to give the largest bandwidth responses and good surface wave efficiencies [2]. Many designs consisting of different geometries have been introduced in literature [3]. A probe fed stacked square patch slotted wideband microstrip antenna is presented [4-5]. An asymmetrical complementary split ring resonator (CSRR) loaded stacked microstrip patch antenna is introduced for broadband applications in [6]. The shape of the patch is formed into a rose leaf and fed with a capacitive coupled rectangular feed in [7]. With the rose leaf structure, impedance bandwidth performance of the antenna is increased up to 69%. Stacked patch antennas have been implemented in low temperature cofired ceramic (LTCC), as well [8-10]. Array examples of stacked patches are also presented [11-14]. In order to obtain broadband characteristic, a patch array is arranged as a three stacked structure consisting of one radiation patch and two parasitic patches [11]. An array configuration of 16 element 45^{o} polarized stacked patches in LTCC is designed for fifth-generation (5G) applications [12]. A 16-element linear polarized stacked patch array and its feeding network is demonstrated for Ku-band applications [13]. A phased array consisting of 32 circularly polarized stacked patch antennas is used to enhance the bandwidth characteristics of commercial drones [14].

Mutual coupling effect between antenna elements is a critical issue in the design of microstrip arrays. This effect may lead to impedance mismatch, decrease in gain, increase in side lobe level (SLL) and occurrence of scanning blindness [15]. Electromagnetic bandgap (EBG) structures that create a photonic crystal to suppress the surface-wave propagation were developed to eliminate mutual coupling and prevent the degradation in radiation performance of the array [16-18].

Defected ground structures (DGS) have been proposed to improve mutual coupling between patch elements [15, 19]. The effect of DGS on coupling characteristics is observed by means of a two element microstrip array and the positive impact of the DGS on mutual coupling is investigated in [19]. However,

Submitted On: October 26, 2020
Accepted On: January 24, 2021
https://doi.org/10.47037/2020.ACES.J.360307

existence of DGS resulted in higher back lobe level of the array pattern. The backward radiation is a critical problem that may cause breakdown of the front-end circuits that are integrated behind the antenna. Besides, the back lobe radiation results in multipath signal propagation that may lead to error in differential positioning systems. The coverage capacity of a base station antenna may also be affected due to the overlapping areas between adjacent sectors [20-21]. Various techniques such as ground plane edge shaping, using a semi-transparent ground plane or isolated soft surface structure and optimizing reflector shape have been applied for the suppression of back lobes in literature [21-26]. [21-25] have been specifically applied to microstrip antennas. Besides, some antennas are introduced as candidates with high FBR values. These include circularly polarized antenna [27], short microstrip leaky-wave antenna [28] and substrate integrated waveguide slot antenna [29]. Various antenna array structures also proposed for improving FBR in broad frequency band [30-32]. A suppressed back-lobe substrate-integrated waveguide slot array antenna is presented for X-band [30]. In [31] a microstrip antenna array with DGS structure is proposed for back lobe reduction. In [32], a mode superposed microstrip patch antenna with bandgap structures is introduced to improve the FBR.

In the above mentioned works, the back radiation is investigated for the radiation of the antenna in broadside direction. However, for a phased array, back lobe generation is observed for all scanning angles. On this ground, in this work, we proposed an asymmetric array structure as an advantageous solution for the broadband phased arrays with concerns in particular wide-scan ranging with suppressed back lobe characteristics, compactness and suitable for simple manufacturing process. The dimensions of asymmetric array structure are investigated by a parametric analysis of substrate size. The proposed stacked patch asymmetric phased array architecture is applied to X-band. With a linear array consisting of 8-elements, $\pm 40^{o}$ beam scanning is observed with less than 1.34 dB scanning loss in the whole 8-10 GHz frequency band. FBR is observed above 30 dB for broadside radiation. Up to $\pm 40^{o}$, the back lobe is suppressed more than 20 dB.

The structure of stacked microstrip antenna and its radiation characteristics are introduced in Section II. Also, its radiation performance is compared with that of traditional microstrip antenna. In Section III, an asymmetrical phased array consisting of stacked patches is demonstrated and its back lobe suppression is observed in terms of scanning angle. In Section IV, experimental verification of the fabricated array prototype is given. Finally, Section VI concludes the paper.

II. DESIGN OF WIDEBAND MICROSTRIP ANTENNA

Stacked structure consists of a ground plane at the bottom layer. A dielectric layer with the radiating patch element is placed above the ground plane. A stacked layer and a parasitic patch are planted as the top layer. The structure of the stacked patch antenna is shown in Fig. 1 together with its design parameters. The stacked patch antenna is fed by a coaxial line whose impedance is $50\ \Omega$. The lower patch is etched on a Rogers 4003C substrate ($\tan\delta = 0.0027$ at 10 GHz) with 35 μm copper thickness, whereas the upper patch is etched on foam ($\tan\delta \cong 0.001$ at 10 GHz) to reduce loss due to surface waves and widen the bandwidth of the antenna. The main beam radiation of the antenna is orthogonal to x-y plane. All dimensions of the stacked patch antenna are listed in Table 1.

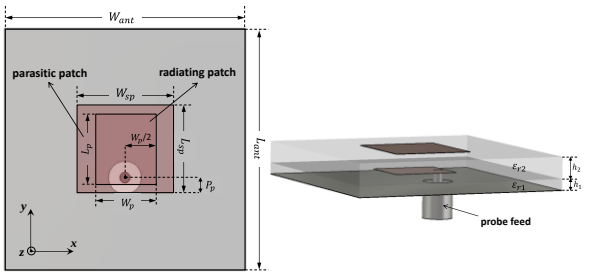

(a) (b)

Fig. 1. Stacked patch antenna: (a) top view; (b) lateral view.

Table 1: Broadband stacked patch antenna dimensions

Parameter	Dimension
ε_{r1}	3.38
ε_{r2}	1.07
W_{ant}	30 mm
L_{ant}	30 mm
W_{sp}	12 mm
L_{sp}	11 mm
W_p	7.5 mm
$\boldsymbol{P_p}$	**2 mm**
L_p	9 mm
h_1	1.52 mm
h_2	3 mm

The numerical analysis of the designed antennas in the paper is accomplished with a three dimensional (3D) full-wave electromagnetic solver, CST Microwave Studio [33]. To demonstrate the superior performance of the stacked patch, results are compared with that of an ordinary patch antenna whose dimensions and material is exactly same with the radiating patch and lower substrate of the stacked patch antenna. Thus, the size and material

details for this structure can also be found in Table 1. In Fig. 2 (a), reflection coefficient variations of the ordinary patch and stacked patch antennas are given as the function of frequency. The bandwidth of the patch antenna covers a 320 MHz band between 8.28-8.6 GHz. The S_{11} variation of the stacked patch antenna is lower than -10 dB for the whole band of interest. This figure clearly demonstrates the broadband characteristic of the stacked structure. The gain and total efficiency variation of the antennas are given in Fig. 2 (b) and Fig. 2 (c), respectively. More than 1 dB gain enhancement and total efficiency above 90% is obtained with the stacked structure in the whole 8-10 GHz band.

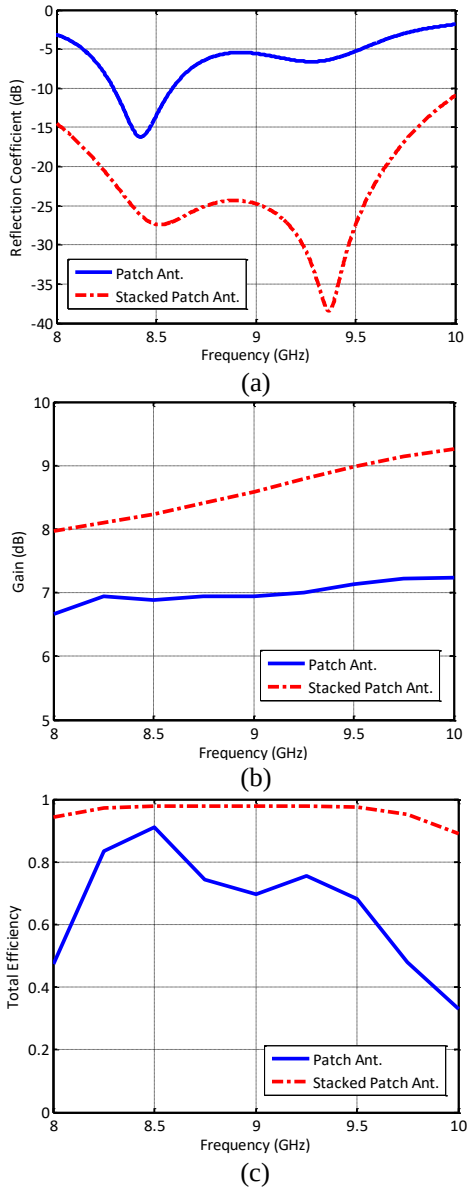

Fig. 2. Performance comparison of stacked patch antenna and ordinary patch antenna: (a) reflection coefficient; (b) gain; (c) total efficiency.

The simulated co-polarized gain patterns are given in Fig. 3 in E- and H-planes at 8 GHz, 9 GHz and 10 GHz. The main beam radiation is observed along z-axis. Shape of the pattern does not change significantly in $\emptyset = 0$ plane. On the hand, the beam in $\emptyset = 90^0$ plane narrows with increasing frequency.

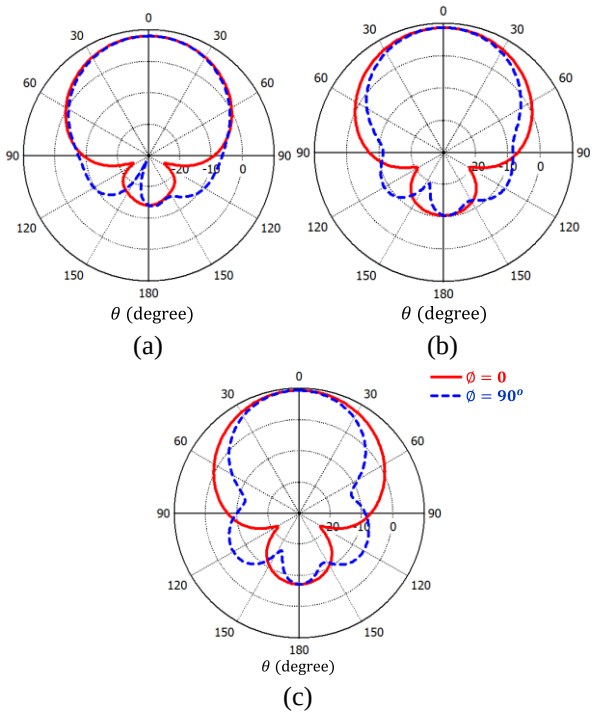

Fig. 3. Gain patterns of stacked patch antenna: (a) 8 GHz, (b) 9 GHz, and (c) 10 GHz.

III. X-BAND PHASED ARRAY DESIGN

Phased arrays are capable of electronically scanning the beam in a predefined angular range with predefined beam characteristics by adjusting the excitation phase and amplitude of the antenna elements. The level of mutual coupling between antenna elements is related with the relative positions of the elements. The dominant surface wave mode couples more strongly compared to other modes in the E-plane. Since the amount of coupling varies with different scan angles, the input impedance of the array will vary with the scanning angle, as well.

In radar applications, planar phased array topologies capable of scanning the space in a single plane are widely required. Automotive radars that scan the horizontal plane within the $\pm 30^o$ scanning angle can be given as an example. In this section, two demonstrations for the linear phased array are given. They both use stacked patch antenna elements and scan the beam in $\pm 40^o$ scanning angle with low scanning loss. The major difference between two examples is their structure. One of them has patch antenna elements placed to the substrate with equal distance from the edges. In the

other one, the patch is placed with unequal distances from the edges. We call this one as asymmetric structure. Asymmetrical structure of the array improves the radiation characteristics of the array, especially reduces the back lobe radiation. Suppression of the back lobe is a critical issue in radars, since its existence may deteriorate the front end circuit of the radar.

A. X-Band linear phased array design

Two linear phased arrays consisting of wide-band stacked patch antenna elements are demonstrated in this section. Stacked patch antenna radiation characteristics are given in Section 2. The distance between antenna elements d, is calculated with $d_{max} = \lambda_c/(1 + |\sin\theta|)$ to avoid grating lobe generation. Here, θ is the beam scanning angle. By setting $\theta = 40^o$, d is determined as $20\,mm$ which is smaller than half wavelength at the lowest frequency of the band. Symmetric and asymmetric stacked patch phased array structures are given in Fig. 4. The lower patch is etched on Rogers 4003C substrate ($\varepsilon_{r1} = 3.38$) and the upper patch is etched on foam ($\varepsilon_{r2} = 1.07$). The patches of the array given in Fig. 4 (a) have been centered to the substrate of the array. To reduce diffraction effect, the substrate size of the array is increased as given in Fig. 4 (b).

Front to back ratio of the asymmetric antenna array structure is investigated by a parametric analysis of substrate size. During this study each parameter (W_1,W_2) is varied alone while the other one is held fixed. The influence of the variables W_1 and W_2 in the antenna array back lobe radiation is summarized in Table 2 and Table 3. It is clear from these tables that highest FBR values are obtained for W_1 to W_2 ratio of 2:1 at the whole operation frequency band.

Table 2: The FBR variations with W_2 when W_1 value is fixed to 13.5 mm

FBR (dB)		W_2 (mm)				
		13.5	20	27	33.5	40.5
W_1 = 13.5 (mm)	8 GHz	17.4	20.3	26.7	19.9	16.8
	9 GHz	17.9	20	24.8	18.6	18
	10 GHz	16.7	19	23.7	18.5	18

Table 3: The FBR variations with W_1 when W_2 value is fixed to 13.5 mm

FBR (dB)		W_1 (mm)				
		13.5	20	27	33.5	40.5
W_2 = 13.5(mm)	8 GHz	17.4	20.2	28.3	23.9	18.4
	9 GHz	17.9	20.7	34	22.2	20
	10 GHz	16.7	18.7	36.2	21.5	18.8

As a result, backward radiation is suppressed. The patches of the asymmetric structure are located 2:1 ratio from the lateral sides of the array. Also, wider spacing is left at the right and left edges of array. The dimensions of the two structures are listed in Table 4.

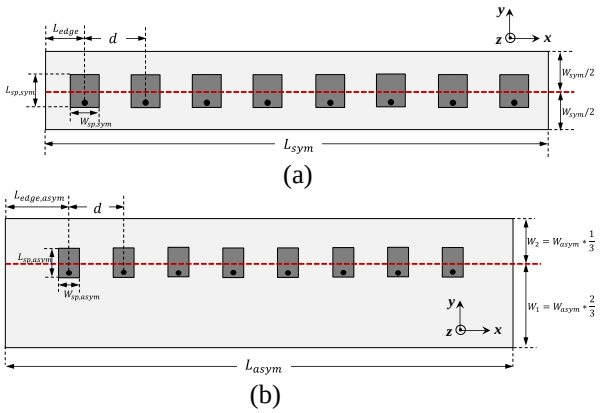

Fig. 4. Stacked microstrip phased array: (a) symmetric; (b) asymmetric configuration.

Table 4: Broadband stacked microstrip phased array dimensions

Symmetric Configuration		Asymmetric Configuration	
Parameter	**Dimension(mm)**	**Parameter**	**Dimension(mm)**
W_{sym}	27	W_{asym}	40.5
L_{sym}	168	L_{asym}	190
d	20	d	20
L_{edge}	14	$L_{edge,asym}$	25
$W_{sp,sym}$	12	$W_{sp,asym}$	12
$L_{sp,sym}$	11	$L_{sp,asym}$	11

B. Simulation results

The array factor (AF) of an N-element linear array placed along *x*-axis can be expressed as:

$$AF = \sum_{n=1}^{N} e^{j(n-1)\psi}, \quad (1)$$

where, $\psi = kdsin\theta cos\emptyset + \beta$. Here, d is the distance between antenna elements, θ is the beam scanning angle and k is the free space wavenumber. The excitation phases of the antenna elements of the linear array are calculated by using $\beta = -kdsin\theta cos\emptyset$ formula since the antenna elements are placed along *x*-axis. It should be noted that the beam of the array is scanning in the x-z plane, thus $\emptyset = 0$ in this plane.

Non-uniform amplitude distribution is preferred to obtain lower namely, -30 dB side lobe levels. Corresponding Dolph-Chebyshev amplitude values are listed in Table 5. The overall size of the symmetrical phased array is $27mm \times 168\,mm$. On the other hand, asymmetrical phased array has $40.5mm \times 190mm$ real estate area.

Active reflection coefficient, Γ_{m} defines the ratio of reflected power when all the antenna elements are simultaneously excited. It can be calculated by Eq. (2) for unequal phase and amplitude excitations:

$$\Gamma_{\mathrm{m}}(\theta) = \sum_{n=1}^{N} S_{mn}\, e^{-jknd\sin\theta}, \quad (2)$$

where $k = 2\pi/\lambda$, m is the index indicating the mth array element and S_{mn} is the transmission coefficient from

port n to port m. The mutual coupling between antenna elements is considered in this equation. Active S-parameters of the symmetric and asymmetric 8 element phased arrays when the beam is steered to $\theta = 40^o$ are given in Fig. 5. Higher values of reflection coefficient are observed for the elements in the middle of the array. $S_{active,j}$ is lower than -10 dB for all j values except $j = 4$. Although $S_{active,4}$ reaches approximately to -9 dB at the lowest frequency of the band for symmetric structure and at the highest frequency of the band for asymmetric structure, its level is still acceptable.

Table 5: Dolph-Chebychev function amplitude values for the linear array

Amplitude #	Value
A_1	0.2622
A_2	0.5187
A_3	0.812
A_4	1
A_5	1
A_6	0.812
A_7	0.5187
A_8	0.2622

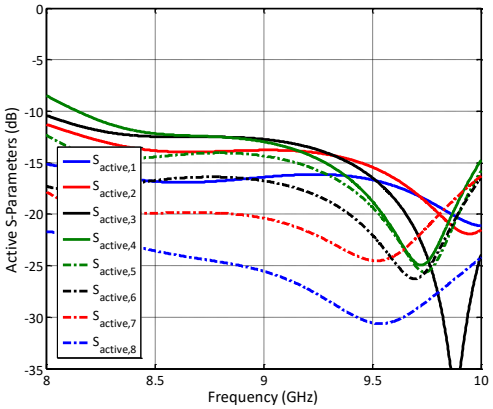

(a)

(b)

Fig. 5. Simulated active S-parameters of a 8-element stacked microstrip phased array radiating to $\theta = 40^o$: (a) symmetric; (b) asymmetric configuration.

Reducing back lobe radiation is critical for radar and base station antenna arrays. Back lobe radiation can be suppressed by using a low back lobe antenna. To increase the subscriber capacity, FBR is expected to be more than 20 dB [26]. The radiation patterns of the symmetrical and asymmetrical arrays at 8 GHz are given in Fig. 6 (a) and Fig. 6 (b), respectively. The patterns are demonstrated up to 40^oscanning angle. The amplitude of array element excitations is listed in Table 5, whereas their relative phases are listed in Appendix I.

For the symmetric stacked patch phased array, 17.14 dB FBR is observed at broadside direction at 8GHz. It decreases to 14.06 dB when the beam is steered to 40^o. The scanning loss for steering the beam to 40^o is 0.54 dB. For the asymmetric structure, FBR is more than 30 dB for broadside radiation and 20.1 dB for 40^oscanning. There is almost no scanning loss for this structure. These figures clearly demonstrate the positive effect of asymmetric placement of the patches on the FBR. Similar conclusions are observed for the patterns at 9 and 10 GHz in Fig. 7 and Fig. 8, respectively. By altering the dimensions of substrate of the array, FBR is increased above 20 dB for all scanning angles at all frequencies. The scanning loss of symmetric structure for steering the beam to 40^o at 9 and 10 GHz are 0.9 dB and 2.19 dB, respectively. It is 0.1 dB and 1.34 dB for the asymmetric structure. Thus, asymmetric structure has positive effect on the scanning loss, as well.

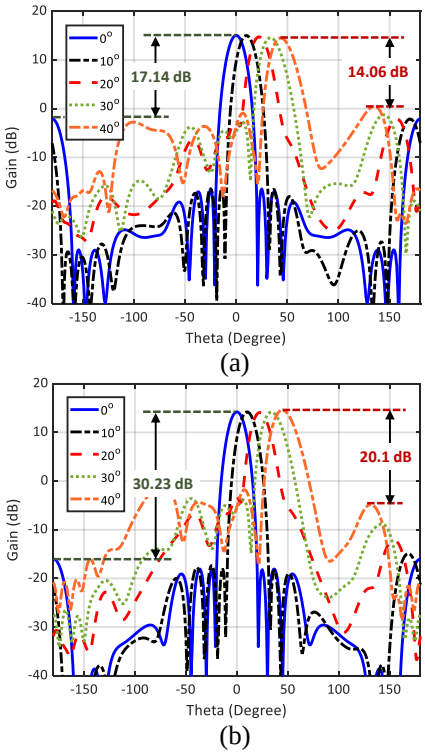

(a)

(b)

Fig. 6. Scanning performance of phased arrays at 8 GHz: (a) symmetric; (b) asymmetric array.

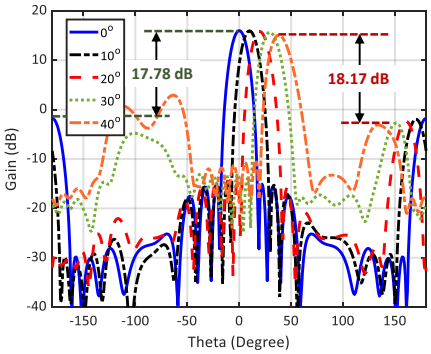

(a)

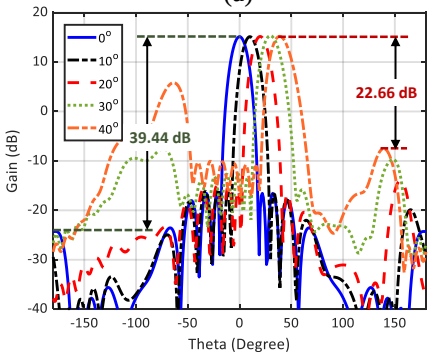

(b)

Fig. 7. Scanning performance of phased arrays at 9 GHz: (a) symmetric; (b) asymmetric array.

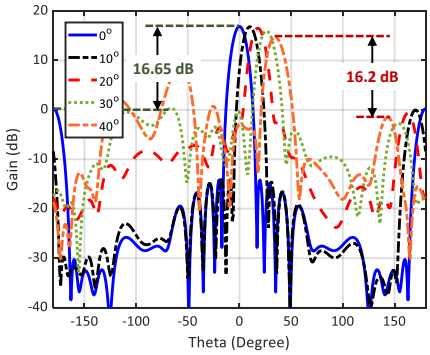

(a)

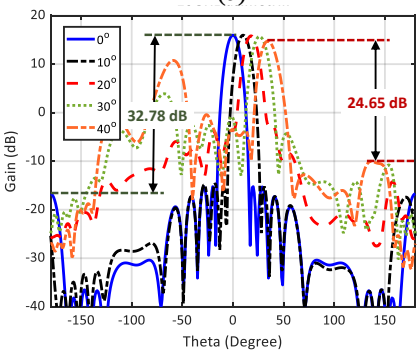

(b)

Fig. 8. Scanning performance of phased arrays at 10 GHz: (a) symmetric; (b) asymmetric array.

IV. EXPERIMENTAL CHARACTERIZATION AND ANALYSIS

For the easy fabrication, a radome layer is added to the array as the top layer. It is Rogers 5880 substrate ($\tan\delta = 0.0009$ at 10 GHz) with 0.254 mm thickness. The dielectric constant of the radome substrate is $\varepsilon_r = 2.2$. The parasitic patches are positioned to the bottom side of the radome as shown in Fig.9 (a). Foam with 3mm thickness is placed under this layer. Below foam layer, there are radiating patches on Rogers 4003C substrate as shown in Fig. 9 (b). By gluing these layers, the asymmetric stacked patch array is constructed. The side view of the fabricated prototype is shown in Fig. 9 (c). SMA connectors that operate up to 18 GHz are soldered to the radiating patches.

(a)

(b)

(c)

Fig. 9. Layers of the asymmetric stacked patch array prototype: (a) bottom view of Rogers 5880 radome layer; (b) top view of Rogers 4003C substrate; (c) side view of the stacked patch array. Foam with 3mm thickness is placed between these two layers.

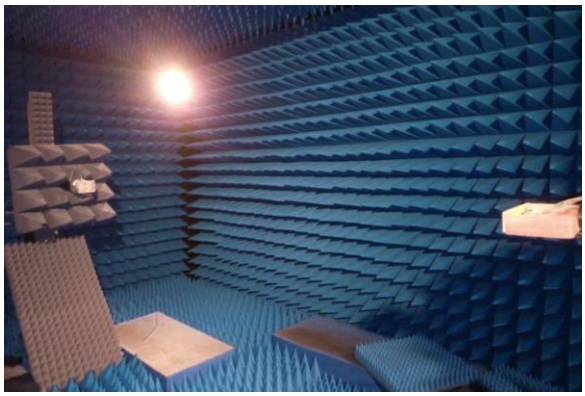

Fig. 10. Measurement setup of the asymmetric stacked patch array in the anechoic chamber.

1×8 RF divider is used for the amplitude excitations of the antenna elements. Fabricated asymmetric stacked patch array is measured in an anechoic chamber. The measurements are performed with 1° resolution at $\phi = 0°$ plane between $-180^o \leq \theta \leq 180^o$. Measurement setup of the array is shown in Fig. 10. The array is measured for the broadside radiation.

Measured active S-parameters of the 8-element asymmetric stacked microstrip phased array is given in Fig. 11 for the case when the array is radiating to $\theta = 0^o$. Ripples are observed in the active S-parameter curves due to the external reflections in the measurement setup. Although existence of ripples is clearly observed, the characteristics of these parameters exhibit similar characteristics with the simulated ones. Measured active S-Parameters show good impedance matching performance within 8-10 GHz band.

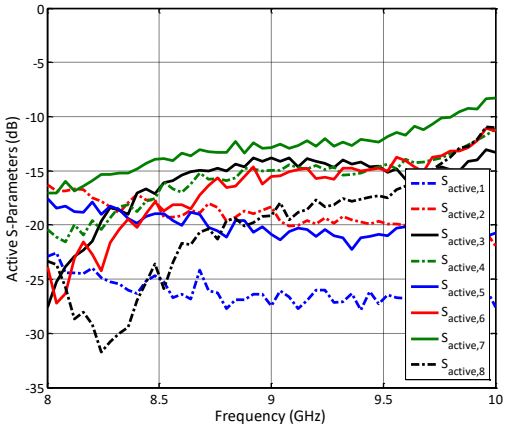

Fig. 11. Measured active S-parameters of the 8-element asymmetric phased array radiating to $\theta = 0^o$.

Table 6: Comparison of proposed structure with references

Reference	Technique	Frequency	FBR improvement (dB)
[30]	Planar choke	9.45-10.30 GHz	>20 dB
[31]	Partial ground and DGS	9.1 GHz	> 6 dB
[32]	EBG structure as a reflector	4.90-5.42 GHz	> 5 dB
Present paper	Asymmetric structure	8-10 GHz	> 20 dB

Measured and simulated normalized co- and cross-pol radiation patterns for broadside radiation are given in Fig.12. Uniform amplitude excitations are used. The simulated and measured patterns are in a good agreement. FBR of 42.06 dB, 45.3 dB and 38.72 dB are observed for the measured patterns of 8 GHz, 9 GHz and 10 GHz, respectively. The peak gain is measured as 10.25 dBi, 12.364 dBi and 10.93 dBi. Effectiveness of using asymmetric structure is clearly observed in the co-pol patterns of simulated and measured array. Table 6 shows the comparisons of our proposed array structure with several published works. These results show that the prosed asymmetric structure improves FBR better than the techniques of previous works in broad frequency band [30-32].

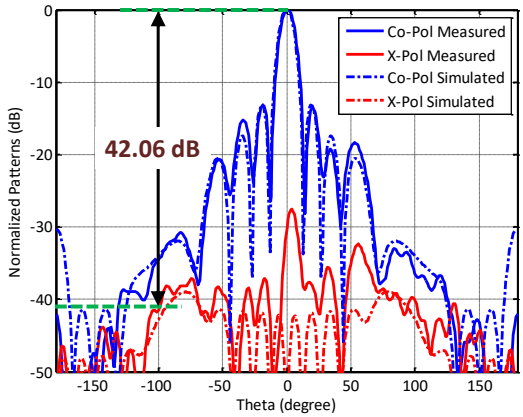

(a)

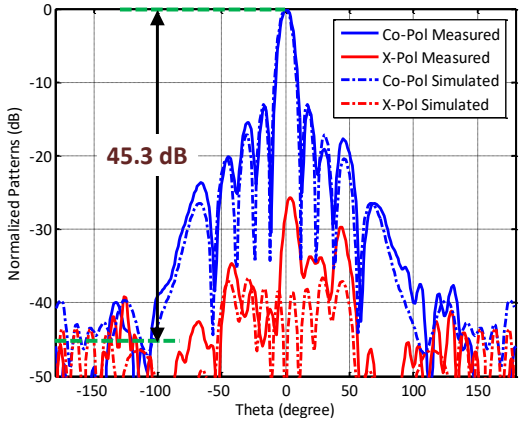

(b)

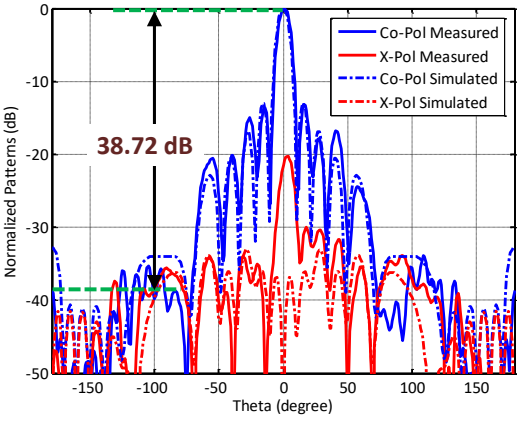

(c)

Fig. 12. Measured and simulated normalized co- and cross-pol radiation patterns for broadside radiation: (a) 8 GHz; (b) 9 GHz; (c) 10 GHz.

V. CONCLUSION

Stacked geometries are widely used to enhance the impedance matching characteristics of the microstrip antenna. In this work, stacked microstrip antenna consisting of foam and radome layers is used as the antenna elements of a broadband phased array. The array is designed to scan the beam in horizontal plane at $-40^o \leq \theta \leq 40^o$ angular range. By altering the physical size of the substrate materials, back lobe suppression is achieved. FBR values that are more than 38 dB is achieved for broadside radiation. It is above 20 dB when the beam is steered to $\theta = 40^o$. Besides, its scanning loss is lower for all steering angles at all frequencies compared to its symmetrical counterpart. Asymmetrical stacked patch phased array prototype is fabricated and measured. Very high FBR is observed in the measurements, as well. With its broadband, high FBR and low scanning loss, asymmetrical stacked patch phased array is suitable as radar and base station antenna.

APPENDIX

Table App.I: Phase excitation values for the stacked microstrip phased array

θ	β_1	β_2	β_3	β_4	β_5	β_6	β_7	β_8
0	**0**	**0**	**0**	**0**	**0**	**0**	**0**	**0**
10^o	**0**	**-37.5**	**-75**	**-112**	**-150**	**-187.5**	**-225**	**-262.5**
20^o	**0**	**-73.8**	**-147.6**	**-221.4**	**-295.2**	**-9**	**-82.8**	**-156.6**
30^o	**0**	**-108**	**-216**	**-324**	**-72**	**-180**	**-288**	**-36**
40^o	**0**	**-138.8**	**-277.6**	**-56.4**	**-195.2**	**-334**	**-112.8**	**-251.6**

θ is the beam scanning angle. All units are in degrees.

REFERENCES

[1] R. B. Waterhouse, "Design of probe-fed stacked patches," *IEEE Trans. Antennas Propagat.*, vol. 47, no. 12, pp. 1780-1784, Dec. 1999.

[2] R. B. Waterhouse, "Stacked patches using high and low dielectric constant material combinations," *IEEE Trans. Antennas Propagat.*, vol. 47, no. 12, pp. 1767-1771, Dec. 1999.

[3] K. Klionovski and A. Shamim, "Physically connected stacked patch antenna design with 100% bandwidth," *IEEE Antennas and Wireless Propagat. Lett.*, vol. 16, pp. 3208-3211, Nov. 2017.

[4] P. K. Singhal, B. Dhaniram, and S. Banerjee, "A stacked square patch slotted broadband microstrip antenna," *Journal of Microwaves and Opto-electronics*, vol. 3, no. 2, pp. 60-66, Aug. 2003.

[5] M. A. Matin, B. S. Sharif, and C. C. Tsimenidis, "Probe fed stacked patch antenna for wideband applications," *IEEE Trans. Antennas Propag.*, vol. 55, no. 8, pp. 2385-2388, Aug. 2007.

[6] M. C. Tang, T. Shi, H. Xiong, and S. Qing, "Low-profile asymmetrical CSRR loaded stacked microstrip patch antenna," *Applied Computational Electromagnetics Society Journal*, vol. 30, no. 8, pp. 850-854, Aug. 2015.

[7] A. A. Lotfi Neyestanak, "Ultra wideband rose leaf microstrip patch antenna," *Progress in Electromagnetics Research*, vol. 86, pp. 155-168, Oct. 2008.

[8] A. Bhutani, H. Bulan, B. Goettel, C. Heine, T. Thelemann, M. Pauli, and T. Zwick, "122 GHz aperture-coupled stacked patch microstrip antenna in LTCC technology," *European Conf. Antennas & Propag. (EuCAP)*, Davos, pp. 1-5, 2016.

[9] A. Panther, A. Petosa, M. G. Stubbs, and K. Kautio, "A wideband array of stacked patch antennas using embedded air cavities in LTCC," *IEEE Microw. Wireless Compon. Lett.*, vol. 15, no. 12, pp. 916-918, Dec. 2005.

[10] W. Hong, A. Goudelev, K. H. Baek, V. Arkhipenkov, and J. Lee, "24-element antenna-in-package for stationary 60-GHz communication scenarios," *IEEE Antennas Wireless Propag. Lett.*, vol. 10, pp. 738-741, July 2011.

[11] H. S. Noh and U. H. Park, "Three-stacked microstrip patch array antenna for both transmitting and receiving," *IEE Proc. Microw. Antennas Propag.*, vol. 153, no. 4, pp. 385-388, Aug. 2006.

[12] G. Guo, L. S. Wu, Y. P. Zhang, and J. F. Mao, "Stacked patch array in LTCC for 28 GHz antenna in-package applications," *2017 IEEE Elect. Design of Adv. Packaging and Systems Symposium (EDAPS)*, Haining, China, Dec. 14-16, 2017.

[13] E. García-Marín, J. L. Masa-Campos, and P. Sánchez-Olivares, "4 x 4 stacked patch array with SIW and microstrip corporate feeding network for Ku-band," *2016 10th European Conference on Antennas and Propagation (EuCAP)*, Davos, Switzerland, Apr. 10-15, 2016.

[14] M. S. Khan, A. Iftikhar, S. A. Naqvi, B. Ijaz, A. Fida, R. M. Shubair, and S. A. Khan, "Circularly polarized 4× 8 stacked patch antenna phased array with enhanced bandwidth for commercial drones," *Int. J. RF Microw. Comput. Aided Eng.*, vol. 30, no. 3, Mar. 2020.

[15] S. Xiao, M. C. Tang, Y. Y. Bai, S. Gao, and B. Z. Wang, "Mutual coupling suppression in microstrip array using defected ground structure," *IET Microw. Antennas Propag.*, vol. 5, no. 12, pp. 1488-1494, Sep. 2011.

[16] G. Ramon, P. Maagt, and M. Sorolla, "Enhanced patch-antenna performance by suppression surface waves using photonic-bandgap substrates," *IEEE Trans. Microw. Theory Tech.*, vol. 47, no. 11, pp. 2131-2138, Nov. 1999.

[17] H. Y. Yang, N. G. Alexopoulos, and E. Yablonovitch, "Photonic band-gap materials for high-gain printed circuit antennas," *IEEE Trans. Antennas Propag.*, vol. 45, no. 1, pp. 185-187, Jan. 1997.

[18] L. Yang, M. Y. Fan, F. L. Chen, J. Z. She, and Z. H. Feng, "A novel compact electromagnetic

bandgap structure and its applications for microwave circuits," *IEEE Trans. Microw. Theory Tech.*, vol. 53, no. 1, pp. 183-190, Jan. 2005.

[19] M. Salehi and A. Tavakoli, "A novel low mutual coupling microstrip antenna array design using defected ground structure," *Int. J. Electron. Commun*., vol. 60, pp. 718-723, Nov. 2006.

[20] E. S. Silveira, D. C. Nascimento, and A. F. Tinoco, "Design of microstrip antenna array with suppressed back lobe," *Journal of Microwaves, Optoelectronics and Electromag. App*., vol. 16, no. 2, pp.460-470, June 2017.

[21] W.G. Lim, H. S. Jang, and J. W. Yu, "New method for back lobe suppression of microstrip patch antenna for GPS," *Proc. of the 40th European Microwave Conf*., Paris, France, pp. 679-682, Nov. 2010.

[22] Y. Li, P. Yang, F. Yang, and S. He, "A method to reduce the back radiation of the folded PIFA antenna with finite ground," *Applied Computational Electromagnetics Society Journal*, vol. 28. no. 2, pp. 110-115, Feb. 2013.

[23] T. J. Cho and H. M. Lee, "Front-to-back ratio improvement of a microstrip patch antenna by ground plane edge shaping," *2010 IEEE Antennas and Propagation Society Int. Symp.*, Toronto, Canada, pp. 1-4, July 2010.

[24] K. Klionovski and A. Shamim, "Back radiation suppression through a semitransparent ground plane for a millimeter-wave patch antenna," *IEEE Trans. Antennas Propag.*, vol. 65, no. 8, pp. 3935-3941, Aug. 2017.

[25] H. M. Lee and J. K. Kim, "Front-to-back ratio improvement of a microstrip patch antenna using an isolated soft surface structure," *Proc. of the 39th European Microwave Conf.*, Rome, Italy, pp. 385-388, Sep. 2009.

[26] Y. Rikuta, H. Arai, and Y. Ebine, "Enhancement of FB ratio for cellular base station antenna by optimizing reflector shape," *IEEE Antennas and Propagat. Society International Symp*., Boston, USA, pp. 456-459, July 2001.

[27] L. Zhang, S. Gao, Q. Luo, P. R. Young, Q. Li, Y.-L Geng, and R. A. Abd-Alhameed, "Single-feed ultra-wideband circularly polarized antenna with enhanced front-to-back ratio," *IEEE Trans. Antennas Propag.*, vol. 64, no. 1, pp. 335-360, Jan. 2016.

[28] Y. L. Chiou, J. W. Wu, J. H. Huang, and C. F. Jou, "Design of short microstrip leaky-wave antenna with suppressed back lobe and increased frequency scanning region," *IEEE Trans. Antennas Propag.*, vol. 57, no. 10, pp. 3329-3333, Oct. 2009.

[29] J. Wei, Z. N. Chen, X. Qing, J. Shi, and J. Xu, "Compact substrate integrated waveguide slot antenna array with low back lobe," *IEEE Antennas Wireless Propag. Lett.*, vol. 12, Aug. 2013.

[30] M. Karami, R. A. Sadeghzadeh, M. Noferesti, and M. Chegeni, "Suppressed back-lobe substrate-integrated waveguide slot array antenna for X-band," *IET Electron. Lett*., vol. 51, no. 11, pp. 811-813, May 2015.

[31] V. N Kumar, M. Satyanarayana, and S. P. Singh, "A novel back lobe reduction technique for microstrip antenna array using partial ground and DGS," *International Journal of Intelligent Engineering and Systems*, vol. 12, no. 2, pp. 182-191, Feb. 2019.

[32] E. Guo, J. Liu, and Y. Long, "A mode superposed microstrip patch antenna and its Yagi array with high front-to-back ratio," *IEEE Transactions on Antennas and Propagation*, vol. 65, no. 12, pp. 7328-7333, Oct. 2017.

[33] CST Microwave Studio, http://www.cst.com, CST GmbH, Darmstadt, Germany.

Melih Türk was born in Ordu, Turkey. He received his B.Sc. degree in Electronics and Communication Engineering from the Kocaeli University in 2011. He received M.Sc. degree in Electronics and Communication Engineering from the Yıldız Technical University in 2019. He is currently working on his Ph.D. in Communication Engineering at the same university. He has been working in the Scientific and Technological Research Council of Turkey (Tubitak) since 2016. Her research interests include radar systems, phase array antennas and RF circuits.

Fikret Tokan received his Ph.D. degree from Yıldız Technical University, Istanbul, in Communication Engineering in 2010. From October 2011 to October 2012, he was Postdoctoral Researcher in the EEMCS Department of Delft University of Technology. From October 2012 to May 2013, he was a Postdoctoral Fellow at the Institute of Electronics and Telecomm. (IETR), University of Rennes 1, France.

Since September 2002, he has been working in the Electromagnetic Fields and Microwave Technique Section of the Electronics and Communications Engineering Department of Yıldız Technical University. He has been currently working as an Assoc. Prof. at that department. His current research interests are UWB antenna design, dielectric lens antennas, reflector systems, electromagnetic waves, propagation, antenna arrays, scattering and numerical methods.